Proceedings of The Institute of Acoustics

"The Use of Matching Layers in the Design of Broadband, High-Efficiency, High-Frequency Transducers Capable of being Operated at Depth"

by H. Koymen*, B. K. Gazey and B. V. Smith,
University of Birmingham, U.K.

*Formerly University of Birmingham.

1.0 INTRODUCTION

An ideal high frequency transducer based upon a half-wave resonant plate as the driving element would have; a high efficiency, a wide fractional bandwidth, high power handling capacity and be capable of operating at large hydrostatic pressures.

These design aims impose the following constraints on the structure.

a) Power absorption in the mounting and any supportive backing must be minimized to obtain high efficiencies.

b) Heavy mechanical damping of the radiating faces is necessary to achieve wide bandwidths.

c) The driving element must be mechanically supported uniformally over its non-radiating surface to allow it to be operated in deep water.

It can be seen that these are conflicting requirements and in particular a) and c) are difficult to realize simultaneously. This has lead to a number of compromise designs employing either pressure compensation of the rear air space, or a supportive backing having a low acoustic impedance whilst retaining a measure of rigidity, e.g. foamed plastics. However, neither of these approaches has proved entirely satisfactory.

Wideband transducers, which incidently also have deep water operational capability, are frequently made using a backing material which has a high acoustic impedance, e.g. epoxy resins loaded with various powdered metals. These designs however have low overall efficiencies because of the large proportion of acoustic power absorbed by the backing. Fig. 1 shows the essential features of a number of simple structures which employ some of the ideas presented above.

This paper presents the results of an investigation into the use of a composite structure comprising a number of resonant sections which is capable of realizing simultaneously all of the desirable characteristics of the ideal transducer. This was achieved by the use of two separate principles. The

first is the synthesis of a backing structure which while being mechanically rigid presents a low impedance to the non-radiating face of the driving element. The second priciple is the elimination of the large acoustic impedance mismatch between the driving element and the water load by the use of a quarter wave matching layer which greatly increases the damping on the radiating face of the element. Similar techniques are available (1,2) for use in medical ultrasonic transducers operating in the 2-3 MHz range.

2.0 COMPOSITE TRANSDUCER STRUCTURES

Fig. 2 shows diagramatically the final composite transducer developed by the authors. This can be divided into three separate basic constant-area components and each is discussed in turn below.

2.1 Driving Element

In addition to the normal thickness resonance, electrostrictive ceramic plates exhibit resonances associated with their lateral dimensions. These are termed 'in plane' resonances and can interfere with the desired piston like motion of the front face. This non-uniformity of surface motion can lead to increased mounting losses when the element is bonded to other layers.

Techniques for reducing the unwanted effects of these intermodal coupling problems include:-

a) The use of a material with a low transverse coupling, such as Lead Metaniobate.

b) Careful selection of the lateral dimensions in relation to the plate thickness.

c) The machining of grooves at strategic points over the surface of the elements to 'break up' the planar modes.

Although various combinations of the above methods were tried it was found in practice (3) that satisfactory composite designs could be realized by using for the driving element a Lead Zirconate Titanate ceramic (PZT) whose lateral dimension to thickness ratio was large, typically greater than 7.5.

2.2 Backing Section

The main objective of the backing is to provide a low acoustic impedance compared with the driving element impedance while providing mechanical support. It is obviously necessary to use solid materials with low elasticities and high compressive strengths. No single solid layer exhibits all of these properties and hence multi-layered resonant structures were used.

The final form of the composite backing structure adopted is shown diagramatically in Fig. 2. This comprises a base of epoxy resin loaded with small air-filled glass balls (Fillite), which has a specific acoustic impedance, Z_B, of around 1.83 M Rayls. Its main function is to provide a low non-reflective terminating impedance, i.e. a resistive termination. To one of its surfaces is bonded a quarter-wave resonant section of steel whose specific acoustic impedance, Z_S, is typically 44.8 M Rayls. This steel layer acts as an impedance transformer creating a high impedance, Z_S^2/Z_B, of the order of 1115 M Rayls at its free surface. This impedance is then transformed to a low value by the use of the second quarter-wave resonant section made of epoxy resin whose specific acoustic impedance, Z_E, is 2.95 M Rayls. Therefore, when this epoxy layer is bonded to the steel layer the transformed impedance at the new free surface becomes $Z_E^2 Z_B/Z_S^2$, which is ideally 0.008 M Rayls. In practice the backing impedance is higher than this because of absorption in the various layers. It is to this final low impedance surface that the rear face of the driving element is bonded.

None of the acoustic impedances for the materials cited above are particularly critical because small variations in Z_S, Z_B and Z_E produce changes in the final impedance which are insignificant compared with the impedance mismatch at the driving element/backing boundary. For example, the typical specific acoustic impedance of PZT-4* is 34.5 M Rayls and hence this mismatch ratio is of the order of 100.

Obviously this combination of solid layers provides the necessary mechanical support for deep water operation.

A typical graph of the measured variation in backing impedance with frequency obtained using a standing wave technique (3) is shown in Fig. 3. The solid curves represent the theoretical predictions. It can be seen that this impedance is less than 0.5 M Rayls over a large fractional bandwidth. This wideband property of the backing is a consequence of the well established wideband characteristics of quarter-wave transformers.

The tolerances in tuning the quarter-wave layers are not critical. Variations in the thickness effect the frequency of minimum impedance of course, but the backing discussed above can tolerate variations of about 10% since it is capable of producing a very low impedance over a frequency range substantially wider than the completed transducer bandwidth.

* Transmitting grade manufactured by Vernitron.

2.3 Front Matching Plate

When radiating into water the Q-factor of a half-wave resonant plate, whether air backed or supported by the synthesised low impedance backing described above, is given by $Q = Z_c/2Z_o$, where Z_c and Z_o are the impedances of the ceramic and water respectively. Typically for PZT-4 this predicts a fractional bandwidth of only 3% and results from the small value of Z_o in relation to Z_c. Z_o can be considerably increased by employing a quarter-wave matching layer between the water load and the front radiating face of the cermic plate. It is worth noting that for the case of the coupling of two semi-infinite media of impedances Z_c and Z_o by a quarter-wave layer of impedance Z_m, the optimum value of Z_m for matching is given by $Z_m = (Z_c\ Z_o)^{\frac{1}{2}}$. However, in the case of interest here one of the media, i.e. the ceramic, is not semi-infinite and is in fact half-wave resonant. Therefore this optimum matching criteria for Z_m is modified.

Probably the simplest technique for deriving this new optimum condition is by treating the quarter-wave section as an approximate parallel resonant circuit (4), as shown in Fig. 4(a). It is now possible to apply simple analogous electric filter techniques to the transducer since, apart from C_o, the clamped capacitance, the combined circuit for the ceramic and matching layers appears as a band-pass filter half-section,as shown in Fig. 4(b), which can be analysed by constant - k techniques, where W is a filter parameter. A full band-pass section can be achieved by tuning the clamped capacitiance, C_o, of the driving element with a parallel inductor, L_e, as shown in Fig. 4(c). For some grades of PZT it is possible to make this full-section symmetrical by the simple addition of a trimming capacitor, C_e, in parallel with the inductor, whereas for other grades a more complicated network is required. For optimum power matching the source impedance of the amplifier, Z_A, must be equal to the transformed load impedance N^2Z_L. Also, these must be equated to the characteristic impedance $(L/C)^{\frac{1}{2}}$, of the filter.

Analysis of this full section filter shows (4) that the optimum impedance, Z_m, for the matching section is given by, $Z_m = (Z_c\ Z_o^2)^{\frac{1}{3}}$. For the case of PZT-4 radiating into water, Z_m equals 4.14M Rayls. A suitable material was synthesized from epoxy resin loaded with an appropriate amount of finely divided magnesium. Techniques for realizing such composite materials have been fully reported elsewhere (5).

3.0 MEASURED PROPERTIES OF PROTOTYPE TRANSDUCERS

Four prototype transducers were made using 5 cm diameter and 6.02 mm thick PZT-4 discs, resonant at 335 kHz. They all had the multilayer low impedance backing and quarter-wave front layer of impedance 4.4 M Rayls. The results of admittance measurements on two of these transducers are shown in Fig. 5 (a) and (b) (the significance of the non-rigid bond will be discussed below). The theoretical predictions were derived using both transmission line and lumped element equivalent circuits. In these calculations the propagation losses in the transformer layers were taken into account. The efficiencies of the two transducers, measured using a radiation balance, are shown in Fig. 5(c).

The fractional bandwidth of around 40% agrees well with the predictions. The main discrepancy arises in the efficiency results. An investigation (3) of the effect of rigid bonds between component layers in composite transducers has shown that a rigid bond can cause a reduction in efficiency of as much as 30% as compared to a fluid bond. The reason for this is considered to be additional losses resulting from the creation of shear stresses at the interfaces due to differential elasticities in the structure and possible non-piston like motion in the driving element. In one of the transducers a 'non-rigid' bond was created between the low impedance backing and the ceramic. This increased the efficiency of the transducer by up to 10%, refer to Fig. 5(c). However, in practice it is not possible to make all the bonds 'fluid' and this is regarded as the main cause of the discrepancy in efficiency measurements.

Fig. 5(d) shows conductance plots of three transducers and the repeatability is obviously good. The small differences are due to slight variations in the tuning of the matching layer. Setting the thickness of this is important if a symmetrical response is to be obtained. In practice the layer was cast 10% oversize and then ground down and tested until the response was symmetrical.

The transducers were also tested at high powers using both C.W. and pulsed signals (3). It was deduced from the C.W. 'soak' tests that intensities of 2 Watts/cm^2 are about the maximum permissible if no permanent damage is to result. In the pulse tests the transducers were driven for about 30 minutes with intensities of around 43 Watts/cm^2, whilst retaining the correct duty cycle such that the C.W. limit was not exceeded. There was no detectable deterioration in the transducer performances as a result of this high stress cycling.

4.0 CONCLUSIONS

A number of composite transducers have been produced which compare very favourably with conventional designs with respect to efficiencies, bandwidths and peak power handling capacity, being solid structures throughout they also have a deep water capability.

Prototypes on test gave measured fractional bandwidths of at least 40%, with efficiencies over this band of never less than 50%. Structures embodying non-rigid bonds would be necessary in order to increase this efficiency figure significantly but they would be less convenient. Through the use of multiple layers on the front face it would be possible to increase the fractional bandwidth slightly but the additional complexity is probably not worth while.

The C.W. power handling capacity of 2 W/cm^2 is rather low resulting from sandwiching the ceramic element between materials of low thermal conductivity. It might be possible to improve this by the inclusion of a heat sink at some suitable surface. However, the pulse power performance is more than adequate for most conventional underwater applications.

5.0 REFERENCES

1. SOUQUET, J. and DEFRANOULD, P.:
'Results on low-loss wideband ultrasonic transducers for non-invasive medical application', Electron. Lett. 1978, 14, 235-236.

2. SOUQUET, J. and DEFRANOULD, P., and DESBOIS, J.:
'Results on low-loss wideband ultrasonic transducers for non-invasive medical application', I.E.E.E. Trans., 1979, SU-26,75-81.

3. KOYMEN, H.: 'Optimisation of the design of high frequency sonar transducers', Ph.D. thesis, Department of Electronic and Electrical Engineering, University of Birmingham, 1979.

4. KOYMEN, H., SMITH, B. V. and GAZEY, B. K.:
'Equivalent circuits for high-frequency sonar transducers', Electron. Lett., 1979, 15, 600-601.

5. PELMORE, J. M.: 'Ultrasonic properties of passive materials for transducer use', Proc. Institute of Acoustics, Birmingham, 1976.

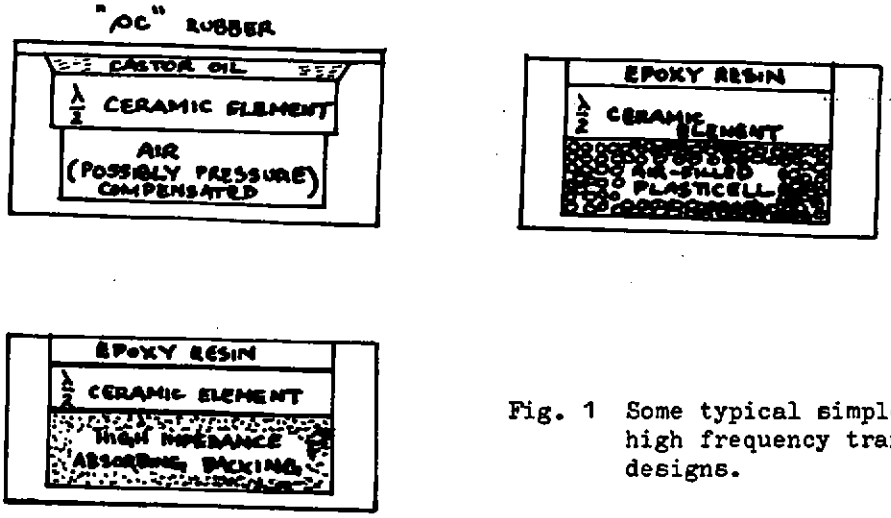

Fig. 1 Some typical simple high frequency transducer designs.

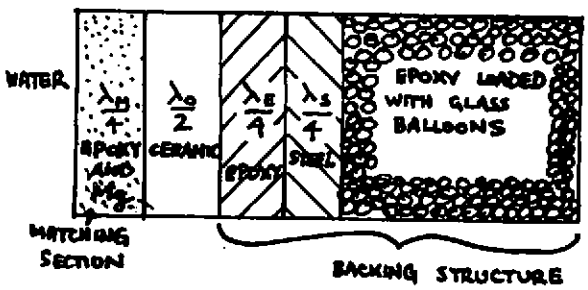

Fig. 2. Composite transducer structure developed by Authors.

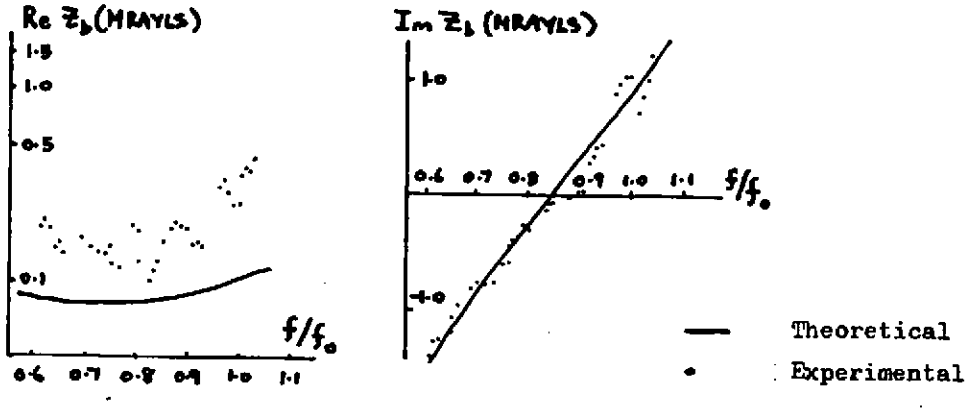

Fig. 3. Acoustic impedance of a transducer backing obtained by double λ/4 transformation, (a) Real part of backing impedance, (b) Imaginary part of backing impedance (Normalised plot).

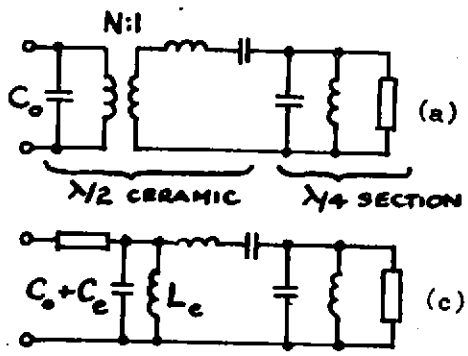

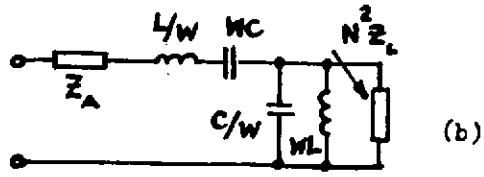

Fig. 4. Bandpass-filter equivalent circuits for matched transducers.

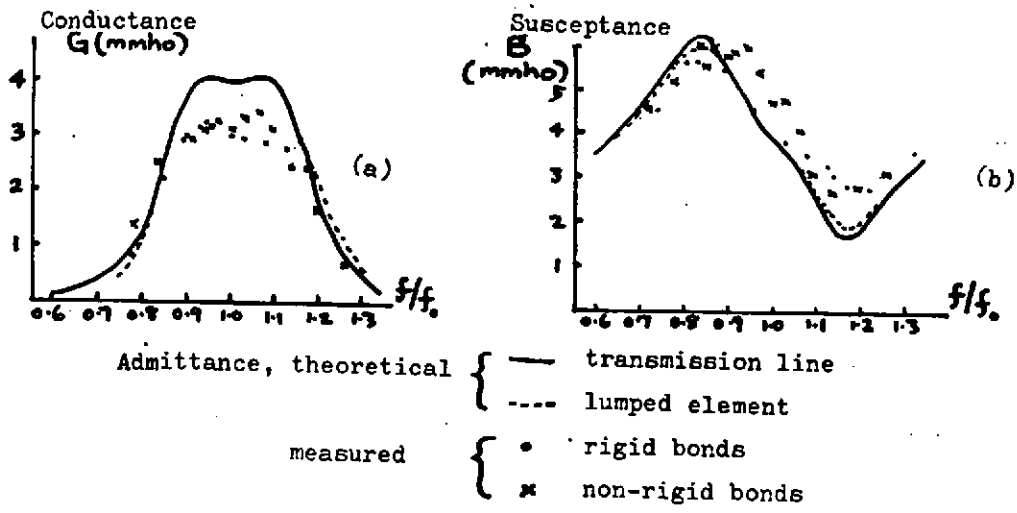

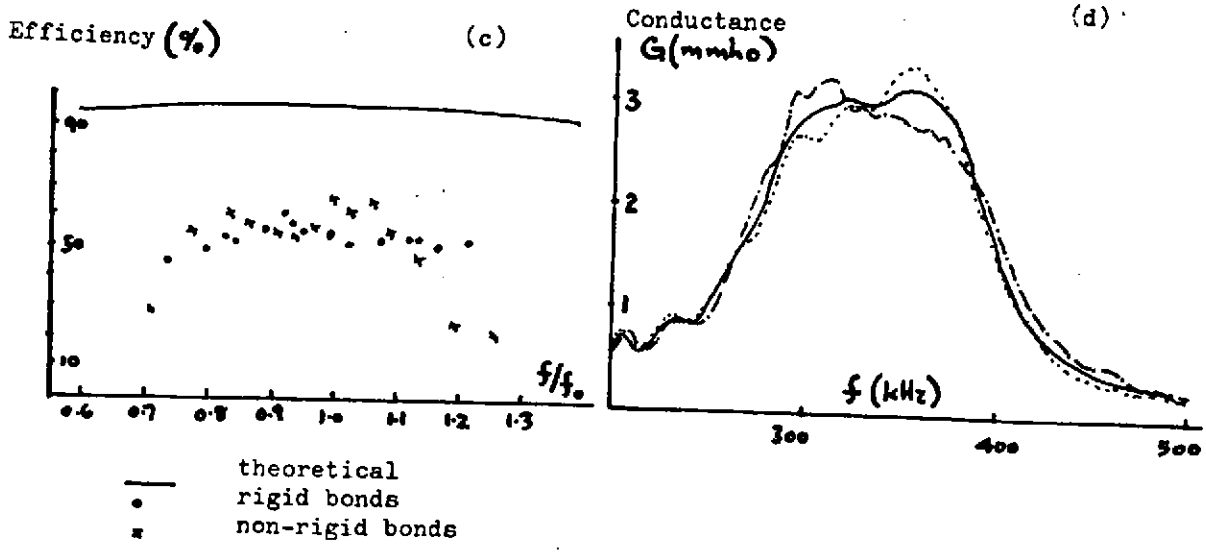

Fig. 5. Experimental results